2010

The height variance range for one frequency fringe pattern profilometry

Yi Ding
University of Wollongong

Jiangtao Xi
University of Wollongong, jiangtao@uow.edu.au

Yanguang Yu
University of Wollongong, yanguang@uow.edu.au

Joe F. Chicharo
University of Wollongong, chicharo@uow.edu.au

Wenqing Cheng
Huazhong University of Science and Technology

Recommended Citation

The height variance range for one frequency fringe pattern profilometry

Abstract

The upper limit on the deepest step of the surface shape that can be accurately determined is an important performance measure associated with the fringe projection profilometry. This metric is evaluated as the variance of height between two adjacent pixels on a fringe patterns reflected from the object surface. This paper presents novel results on this metric based on the Nyquist sampling theorem originally developed in the area of communication theory. Compared to existing results, we indicate that the fringe width and digital image resolution also affect the height variance range significantly. This new result could be used to increase the measurement range for projection system.

Disciplines

Physical Sciences and Mathematics

The height variance range for one frequency fringe pattern profilometry

Yi Ding[1,2], Jiangtao Xi[2], Yanguang Yu[2], Joe Chicharo[2], Wenqing Cheng[1]

[1]Department of Electronic and Information Engineering,
Huazhong University of Science and Technology, Wuhan, 430074, China
[2]School of Electrical, Computer and Telecommunications Engineering
University of Wollongong, Wollongong, NSW 2522, Australia
E-mail:dingyi1688@gmail.com, jiangtao@uow.edu.au

Abstract—**The upper limit on the deepest step of the surface shape that can be accurately determined is an important performance measure associated with the fringe projection profilometry. This metric is evaluated as the variance of height between two adjacent pixels on a fringe patterns reflected from the object surface. This paper presents novel results on this metric based on the Nyquist sampling theorem originally developed in the area of communication theory. Compared to existing results, we indicate that the fringe width and digital image resolution also affect the height variance range significantly. This new result could be used to increase the measurement range for projection system.**

Keywords-Deepest surface step(DSS); the Nyquist sampling theorem; fringe projection profilometry; height variance range

I. INTRODUCTION

Digital fringe projection profilometry (DFPP) is one of the most promising non-contact approaches to measure 3D surface shapes. With DFPP, a frame of image with a particular pattern is projected onto the surface to be measured. The height distribution of the surface deforms the projected fringe patterns, which are captured by a camera from a different angle. When the projected fringes have periodic or sinusoidal patterns, the deformation can be considered as phase modulation and thus retrieving the phase difference between the original and deformed fringe patterns yields the 3D information of the surface. In order to obtain phase maps from original and deformed fringe patterns, a number of fringe pattern analysis methods have been developed, including Fourier transform profilometry (FTP) [1,2,3,4,5,6], phase shifting profilometry (PSP) [7,8,9], spatial phase detection (SPD) [10], phase locked loop (PLL) [11] and other analysis methods [12,13]. Also, a generalized analysis model (GAM) [14,15] has been proposed to describe the relationship between reference pattern and the deformed one in profilometry systems. The measurement accuracy can be greatly improved by GAM when the projected sinusoidal fringe patterns are distorted by unknown factors.

Measurement accuracy and speed are the two major performance metrics associated with 3D shape measurement technology and most research efforts done so far aims to yield improvements on these two metrics. However, another performance measure also important is the upper limit on the complexity of the surface shape that can be measured. As DFPP is based on projection of images using digital projector, the complexity of the surface shape can be evaluated by variance of the height that is, the difference of height between the adjacent pixels. For a particular DFPP system, the maximal height change between the adjacent pixels is usually determined by the spatial width of the fringes. In this paper, this metric is referred to as the deepest surface step (DSS), and evaluation of which will provide an effective way to choose fringe patterns, particularly the spatial width of the fringes.

The very first result on DSS was presented in [2,3] for conventional FTP, in which the DSS was shown to be $\frac{l_0}{3d_0}$, where d_0 is the distance between camera focal point and projector focal point, l_0 is the distance between camera focal point and object surface (Figure 1). In another work [16], a higher DSS, $\frac{l_0}{d_0}$, is achieved by means of adding an extra fringe pattern with a phase shift of π in contrast to the original pattern. These results on DSS are interesting as they depend on the projection geometry only. However, based on our experiment observations, we found that the DSS is also dependent on the width of fringes.

In this paper, we present new results on the DSS that can be achieved by a DFPP system based on a single image with a periodic fringe pattern. As shown by the following sections, the DSS is determined not only by the projection geometry, but also by the fringe pattern and the digital image resolution.

This paper is organized as follows. In Section 2, the existing results on the height variance range for DFPP are presented. In Section 3, the novel height variance range for DFPP is derived based on the Nyquist sampling theorem, and is compared to existing results. Section 4 concludes the paper.

II. EXISTING WORK

A schematic diagram of a typical fringe pattern profilometry (FPP) system is shown in Figure 1. For simplicity, we consider a cross section of object surface for a given y coordinate.

In this case, the intensity of fringe pattern captured by the CCD camera and the height distribution function can be expressed as a function with single variable x.

Figure 1. Schematic diagram of FPP.

We use $s(x)$ and $d(x)$ to denote the intensity of the reference and deformed fringe pattern respectively and use $h(x)$ to represent the height distribution of the object surface. Assuming a periodic fringe pattern is used with T_0 being the period, the fringe pattern can be expressed as:

$$s(x) = \sum_{k=0}^{+\infty} a_k \cos(2\pi k f_0 x + \omega_k) \qquad (1)$$

$$d(x) = \sum_{k=0}^{+\infty} a_k \cos(2\pi k f_0 x + \phi_k(x) + \omega_k)$$

$$= \sum_{k=0}^{+\infty} a_k \cos(2\pi k f_0 x + k\phi(x) + \omega_k) \qquad (2)$$

where f_0 is the spatial fundamental frequency of fringe pattern (note that $T_0 = \dfrac{1}{f_0}$). $\phi(x)$ is the phase shift caused by the object profile, which contains the object height information. a_k is the amplitude of the k-th order harmonics of fringe patterns. $k = 0$ represents the direct current component in $s(x)$ and $d(x)$, $k = 1$ represents the fundamental component in $s(x)$ and $d(x)$. The fundamental component in $s(x)$ and $d(x)$ are used to obtain the phase shift $\phi(x)$ [3,7]. When the phase shift is obtained, the height distribution can be determined by:

$$h(x) = \frac{l_0 \phi(x)}{\phi(x) - 2\pi f_0 d_0} \quad . \qquad (3)$$

From (1) and (2) we can see that the $h(x)$ can be obtained as long as we are able to determine $\phi(x)$, the phase shift in the fundamental component.

In order to work out the DSS, we analyze the frequency feature of deformed fringe pattern. As shown by (2), the fringe patterns are characterized by multiple harmonic structures in spatial frequency domain, and the spatial instantaneous frequency of each harmonic component can be acquired by differentiating the phase with respect to x. The instantaneous frequency of each harmonic component can be written as:

$$f_k(x) = \frac{1}{2\pi} \frac{d(2\pi k f_0 x + k\phi(x) + \omega_k)}{dx} = k f_0 + \frac{k}{2\pi} \frac{d\phi(x)}{dx}$$
$$k = 1, 2, 3 \ldots\ldots N \qquad (4)$$

Figure 2. Axis on schematic diagram of FPP.

When $k = 1$, we have the instantaneous frequency of fundamental component as follows:

$$f_1(x) = f_0 + \frac{1}{2\pi} \frac{d\phi(x)}{dx} \qquad (5)$$

The above equations imply that in contrast to $s(x)$, the deformed fringe pattern $d(x)$ is characterized by frequency modulation (FM) with a frequency deviation $\dfrac{k}{2\pi} \dfrac{d\phi(x)}{dx}$ associated with the k-th order harmonic component. Consequently, $d(x)$ will exhibit a frequency spectrum as shown in Figure 3, consisting of a series of narrow-band components with their central frequencies being the harmonic frequencies, that is, multiple integers of f_0.

The DSS derived in [3] is based on the analysis of the spectrum in Figure 3. The idea is that in order to achieve an accurate measurement, there must not be an overlap between the fundamental component (denoted as Q_1 in Figure 3) and its adjacent ones including Q_0 and Q_2. Based on this constraint, the DSS can be obtained as follows [3]:

$$\left| \frac{d\phi(x)}{dx} \right|_{max} < \frac{2\pi f_0}{3} \qquad (6)$$

Substituting (3) into (5), the height variance range is:

$$\left| \frac{dh(x)}{dx} \right|_{max} < \frac{l_0}{3d_0} \qquad (7)$$

This above result shows that the conventional FTP technique is able to measure the surfaces with their slopes not exceeding $\dfrac{l_0}{3d_0}$.

Figure 3. Deformed spatial frequency spectrum for a given y coordinate.

As shown by Figure 1 and the result in (6), the value of DSS is limited by the spectral width of the DC component (corresponding to the background illumination) and the 2nd order harmonic component Q_2. As an effort to increase the DSS, an improved FTP approach was proposed [16] where two-fringe patterns are combined to eliminate DC and harmonic components. In this case, Q_1 is allowed to spread to zero in the left and to $2f_0$ in the right, yielding the DSS as follows [16]:

$$\left|\frac{dh(x)}{dx}\right|_{max} < \frac{l_0}{d_0} \qquad (8)$$

The result in (8) is obviously better than that in (7), but as mentioned above, the increase in DSS is at the cost of adding an extra image.

III. NEW RESULTS ON DSS

The DSS for FTP using pure sinusoidal fringe patterns is said to be $\frac{l_0}{d_0}$ in [16] as briefed above. However, when we revisit this conclusion, there is one point needing further investigation. That is, the allowable range for Q_1 to spread is not symmetrical with respect to f_0. In other words, the spread is able to extent to zero, but also can extent to a value much higher than $2f_0$. This means that surface with a steeper slope can also be measured without ambiguity.

In order to obtain the range of the DSS, we still utilize the frequency spectrum of the deformed fringe pattern image $d(x)$. Assuming that the image has resolution of N pixels over a distance of L meters in x-direction, the resolution of the image in x-direction is $\frac{N}{L}$ pixels per meter.

Also if the image has M fringes in x-direction, we have $\frac{N}{ML}$ pixels within each fringe. By considering $d(x)$ as a signal, we can say that signal has a sampling frequency $f_s = \frac{N}{L}$ and a fundamental fringe frequency $f_0 = \frac{N}{ML} = \frac{f_s}{M}$.

We employ the Nyquist sampling theorem to obtain DSS. According to the theorem, if a signal $d(x)$ is sampled at the frequency f_s into a discrete sequence, the signal $d(x)$ must have its frequency restricted within the range of $[0, \frac{f_s}{2})$, otherwise the signal can not be reconstructed from the discrete form. Therefore we can say that Q_1 must be within the range $[0, \frac{f_s}{2})$, as seen by Figure 4.

The highest instantaneous frequency of the fundamental frequency component f_{1max} must be less than half of the sampling frequency f_s, so we have:

$$f_{1max} = f_0 + \frac{1}{2\pi}\frac{d\phi(x)}{dx} < \frac{f_s}{2}. \qquad (9)$$

Considering $h(x) = \frac{l_0\phi(x)}{\phi(x) - 2\pi f_0 d_0}$, and assuming that l_0 is much bigger than $h(x)$, we have
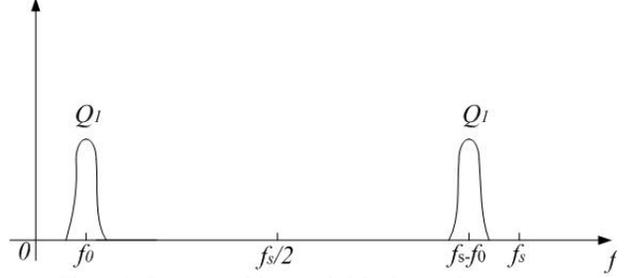

Figure 4. Spectrum of the sampled fundamental component.

$$\frac{h(x)}{l_0} = -\frac{\phi(x)}{2\pi f_0 d_0}, \qquad (10)$$

Differentiating both sides of (10) gives:

$$\frac{d\phi(x)}{dx} = -\frac{2\pi f_0 d_0}{l_0}\frac{dh(x)}{dx}. \qquad (11)$$

Then from (9) and (11), we have:

$$f_0 - \frac{f_0 d_0}{l_0}\frac{dh(x)}{dx} < \frac{f_s}{2}. \qquad (12)$$

This equation indicates that the highest instantaneous fundamental frequency can be extended to $\frac{f_s}{2}$, which is much higher than what proposed in [16] (that is, $2f_0$). From (12) we have:

$$\frac{dh(x)}{dx} > (1 - \frac{f_s}{2f_0})\frac{l_0}{d_0} \qquad (13)$$

At the same time, from (5) and (11) we have:

$$f_1 = f_0 - \frac{f_0 d_0}{l_0}\frac{dh(x)}{dx} = [1 - \frac{d_0}{l_0}\frac{dh(x)}{dx}]f_0. \qquad (14)$$

As f_1 must be bigger than zero, so the lowest instantaneous frequency of fundamental component f_{1min} can be determined by:

$$f_{1min} = [1 - \frac{d_0}{l_0}\frac{dh(x)}{dx}]f_0 > 0 \qquad (15)$$

From (15) we have:

$$\frac{l_0}{d_0} > \frac{dh(x)}{dx} \qquad (16)$$

These equations show the upper and lower bound of the height variance DFPP can measure for the cases when the harmonic components and direct current component are entirely eliminated. By putting the upper and lower bound together we have the following:

$$\frac{l_0}{d_0} > \frac{dh(x)}{dx} > (1 - \frac{f_s}{2f_0})\frac{l_0}{d_0}. \qquad (17)$$

When f_s is four times as f_0, the height variance range is the same as (8), in this regard, our research can explain the result in [16].

The upper bound we acquire is the same as [16], but the absolution of lower bound $\left|(1-\frac{f_s}{2f_0})\frac{l_0}{d_0}\right|$ is much bigger than $\left|\frac{l_0}{d_0}\right|$ given by [16], we can use a numerical example to demonstrate the difference between the upper and the lower bounds. Assuming that $l_0 = 3m$, $d_0 = 1m$, the camera resolution is 1392×1039, and the field of vision of the camera is $260\,mm\times 194\,mm$, the equivalent spatial period of projected fringe pattern is 25.7mm. The spatial sampling frequency is $f_s = \frac{1392}{260}\,l/mm = 5.3538l/mm$ (l/mm means lines per millimeter), and the spatial fundamental frequency is $f_0 = \frac{1}{25.7}\,l/mm = 0.0387l/mm$. Based on (8) given, the height slope range is:

$$3>\frac{dh(x)}{dx}>-3,$$

The slope range given by (17) is:

$$3>\frac{dh(x)}{dx}>-204.5118.$$

As shown by (17), $\frac{dh(x)}{dx}$ has different range when it takes different signs (i.e., positive or negative). Let us consider these two cases as follows.

For the case where $\frac{dh(x)}{dx}$ is positive, implying that the surface goes up alone x (the left rising side surface of the object in Figure 2). As $\frac{l_0}{d_0}>\frac{dh(x)}{dx}>0$, the DSS of rising surfaces of object is $\frac{l_0}{d_0}$. While for the case where $\frac{dh(x)}{dx}$ is negative, that is, the DSS of the object surface going down alone x (which is the right falling surface of the object in Figure 2), we have $0>\frac{dh(x)}{dx}>(1-\frac{f_s}{2f_0})\frac{l_0}{d_0}$, implying that the object with much steeper falling surfaces can still be measured.

From (17) we can see that the height variance range not only depends on the projection geometry, but also on the fundamental fringe pattern and the digital image resolution. It also depends on the slope of the object surfaces. We can extend the measurement range of a projection system by increasing sampling frequency or by decreasing the fundamental frequency.

Since CCD camera captures digital fringe pattern, phase derivation in fact means the phase difference between two adjacent pixels. We hence can use the difference to substitute the phase derivation, thus (5) can be written as:

$$f_1(x) = f_0 + \frac{1}{2\pi}\frac{\Delta\phi(x)}{\Delta x}.$$

Where $\Delta\phi(x)$ denotes the phase difference between any two adjacent pixels, Equation (17) can be rewritten in the following discrete form:

$$\frac{l_0}{d_0} > \frac{\Delta h(x)}{\Delta x} > (1-\frac{f_s}{2f_0})\frac{l_0}{d_0}.$$

As $\Delta x = 1$, the equation can be further written as:

$$\frac{l_0}{d_0} > \Delta h(x) > (1-\frac{f_s}{2f_0})\frac{l_0}{d_0} \qquad (18)$$

$\Delta h(x)$ is the height variance between any two adjacent pixels. Equation (18) gives the range of $\Delta h(x)$, in which the object height information can be acquired without ambiguity.

Let us look at (14) again, which can also be written in the discrete form:

$$f_1 = [1-\frac{d_0}{l_0}\Delta h(x)]f_0 \qquad (19)$$

Equation (19) implies that if we know the approximate range of the object height slope, we can estimate the frequency range of deformed fringe pattern spectrum in spatial frequency domain. The results will be very helpful for the design of a digital band-pass filter in order to pick up the fundamental components and to eliminate the noises in the captured fringe pattern image.

IV.   CONCLUSIONS

We presented new results on the DSS that can be achieved by a DFPP system based on a single image with a periodic fringe pattern. Compared to existing results, the DSS depends not only on the projection geometry, but also on the fringe pattern and the digital image resolution. The results tell us that the measurement range of projection system can be extended by increasing image resolution and adjusting projection geometry. We have also shown that for an object to be measured, its falling surface can be much steeper than its rising surface. In addition, we also found the relationship between height variance and the spread of fundamental frequency component, which is useful for digital filter design in order to eliminate the influence of various noises associated with the DFPP systems.

REFERENCES

[1]   R. Green, J. Walker, and D. Robinson, "Investigation of the Fourier-transform method of fringe pattern analysis," Opticsl and Lasers in Engineering, vol. 8, pp. 29-44, 1988.

[2]   M. Takeda, H. Ina, and S. Kobayashi, "Fourier-transform method of fringe-pattern analysis for computer-based topography and interferometry," Journal of the Optical Society of America A, vol. 72, pp. 156-160, 1982.

[3] M. Takeda, and K. Mutoh, "Fourier transform profilometry for the automatic measurement of 3-D object shapes,", Applied Optics, vol. 22, pp. 3977-3982, 1983.

[4] J. Yi, and S. Huang, "Modified Fourier transform profilometry for the measurement of 3-D steep shapes," Optics and Lasres in Engineering, vol.27, pp. 493-505, 1997.

[5] X. Su, and W. Chen, "Fourier transform profilometry: a review, " Optics and Lasers in Engineering, vol. 35, pp. 263-284, 2001.

[6] X. Su, W. Chen, Q. Zhang, and Y. Chao, "Dynamic 3-D shape measurement method based on FTP," Optics and Lasers in Engineering, vol. 36, pp. 49-64, 2001.

[7] V. Srinivasan, H. Liu, and M. Halioua, "Automated phase measuring profilometry of 3-D diffuse object," Applied Optics, vol. 23, pp. 3105-3108, 1984.

[8] H. Su, J. Li, and X. Su, "Phase algorithm without influence of carrier frequency," Optics Engineering, vol. 36, pp. 1799-1805, 1997.

[9] X. Su, W. Zhou, von Bally, and D. Vukicevic, "Automated phase-measuring profilometry using defocused projection of Ronchi grating," Optics Communications, vol. 94, pp. 561-573, 1992.

[10] S. Toyooka, and Y. Iwaasa, "Automatic profilometry pf 3-D diffuse objects by spatial phase detection," Applied Optics, vol. 25, pp. 1630-1633, 1986.

[11] R. Rodriguez-Vera, and M. Servin, "Phase locked loop profilometry," Optics and Lasers Technology, vol. 26, pp. 393-398, 1994.

[12] A. Moore, and F. Mendoza-Santoyo, "Phase demodulation in the space domain without a fringe carrier," Optics and Lasers in Engineering, vol. 23, pp. 319-330, 1995.

[13] J. Villa, M, Servin, and L. Castillo, "Profilometry for the measurement of 3-D object shapes based on regularized filters," Optics Communications, vol. 161, pp. 13-18, 1999.

[14] Y. Hu, J. Xi, J. Chicharo, E. Li, and Z. Yang, "Discrete cosine tranform based shift estimation for fringe profilometry using generalized analysis model," Applied Optics, vil. 45, pp. 6560-6567, 2006.

[15] Y. Hu, J. Xi, E. Li, J. Chicharo, and Z. Yang, "Inverse function analyasis method for fringe pattern profilometry," IEEE Transactions on Instrumentation and Measurement, vol. 58, pp. 3305-3314, 2009.

[16] J. Li, X. Su, and L. Guo, "Improved Fourier transform profilometry for the automatic measurement of three-dimensinal object shapes," Optical Engineering, vol. 29, pp. 192-198, 2004.